Chapter

Fluid Structure Interaction Study of Stenosed Carotid Artery Considering the Effects of Blood Pressure and Altered Gravity

S.M. Abdul Khader, Nitesh Kumar and Raghuvir Pai

Abstract

Atherosclerosis is a very common cardiovascular disease (CVD) causing increased morbidity. Atherosclerosis is a disease that involves several factors and usually affects the wall of the arterial bifurcations. Advanced Computational Fluid Dynamics (CFD) techniques has the potential to shed more light in understanding of the causes of atherosclerosis and perhaps in its early diagnosis. Fluid Structure Interaction (FSI) study was carried out on two different three dimensional patient specific cases (a) Normal carotid bifurcation and (b) Stenosed carotid bifurcation. Physiological conditions were considered to evaluate hemodynamic parameters and understand the origin and progression of atherosclerosis in the carotid artery bifurcation, first for the normal and then with hypertension disease. Commercial software ANSYS and ANSYS CFX (version 19.0) was used to perform a two-way FSI using a fully implicit second-order backward Euler differencing scheme. Arterial response was calculated by employing an Arbitrary Lagrangian–Eulerian (ALE) formulation and using the temporal blood response. The carotid artery bifurcation caused a velocity reduction and backflow was observed causing a reduction in the shear stress. A low shear stress resulted due to an oscillatory behavior at the start point of the internal carotid artery near the carotid sinus. Shear stresses are obtained by using anatomically realistic 3D geometry and representative physiological conditions. Results of this study agree with those in the literature showing that the regions with low wall shear stress. Geometry and flow conditions greatly affected the hemodynamics of the carotid artery. Furthermore, regions of relatively low wall shear stress were observed post stenosis, which is a known cause of plaque development and progression. Under altered gravity conditions the same artery was studied to determine the flow conditions and predict the progression of plague.

Keywords: fluid structure interaction, stenosis, carotid artery, blood pressure, altered gravity

1. Introduction

The most important and essential system in human body is the cardiovascular system, also known as circulatory system. In the circulatory system, the heart acts as a pump, supplying the blood to different tissues, organs and muscles of the body through the dense network of ducts: arteries and veins. The normal blood flow

through arteries can be altered significantly by arterial diseases such as atherosclerosis [1]. The atherosclerosis is characterized by the thickening, narrowing and stiffening of the arterial walls. The hardened substance along the walls of the arteries is called plaque and the plaque deposit gradually narrows the artery. The artery, hereby loses its flexibility, which ultimately leads to the blockage of the artery [2]. The narrowing of artery will obstruct and severely reduce the blood flow leading to the organ disfunction [3]. The detailed study of the gradual narrowing or bulging of the artery will help in understanding the underlying mechanisms for unusual behavior of blood flow [4]. The fluid mechanical forces due to the interaction of the blood flow and the arterial wall have a strong influence on the initiation and progression of narrowing or bulging of the artery [5]. Detailed study of hemodynamics in stenosis will be useful in the diagnosis and treatment of vascular diseases [6]. Clinically analyzing the hemodynamics will not yield the detailed investigation using current diagnostic imaging options such as angiography, CTA, MRA or duplex scanning [7]. The detailed information about the hemodynamics in diseased vessels can be obtained from the numerical simulations, and such simulations will help in obtaining a better insight in predicting the hemodynamics. It was observed that hemodynamics of the carotid artery was very much affected by the geometry and flow conditions. Furthermore, regions of relatively low wall shear stress were observed post stenosis, which is a known cause of plaque development and progression [8].

Another major cause of stroke is hypertension. Some of the studies have investigated the effect of hypertension on aneurysms and stenosed arteries. Researchers observed that hypertension increases the WSS and deformation in aneurysm regions, which were initiated by extreme stress - strain conditions [9], whereas Milad et al. [10] experimentally elucidated that the increase in stenosis severity in the carotid artery. This observation is found to fluctuate the hemodynamic parameters especially at throat of the stenosis. All the parameters help predict the locations of potential plaque growth and these results helped in studying the plaque growth and arterial remodeling [10]. It is also found that, the effect of hypertension on the atherosclerotic arteries was studied as it poses a major risk in the rupture of the plaque [11]. A significant correlation between carotid strain parameters and peak and mean WSS in hypertension was also observed [11].

Moreover, the numerical study focusing on flow variation due to gravitational effect during change of different postures such as sitting, sleeping and standing have been discussed with more focus on clinical aspects [12]. Some of the studies have justified the variation in flow behavior during change of postures as observed clinically [13]. The analytical models representing the vascular network in order to predict the variation in flow and pressure during change of postures were also developed. [14]. However, most of these studies are investigated for space application with different conditions such zero gravity and hyper gravity [15]. In another attempt, patient specific numerical study is simulated to demonstrate the gravitational effects on the brain circulation under auto-regulation for change of postures [16]. Hence, the influence of gravity also plays a very vital role in studying the detailed blood flow analysis because of constant change of postures.

Overall, these numerical simulations will aid in interpreting the existing *in-vivo* data, and eventually lead to the development of improved imaging techniques [17]. It is also recognized that narrowing or bulging of arteries are closely related with blood flow characteristics, such as areas of flow reversal or low and oscillatory shear stress [18]. Therefore, a detailed understanding of the local hemodynamics can have useful applications, for instance in predicting potential regions for the formation and development of atherosclerosis, or the consequences of surgical intervention [19].

However, the effect of variation in blood pressure on atherosclerosis has been limited and few studies have attempted to predict that hypertension increases the WSS and arterial deformation initiated by extreme stress – strain conditions [20–22]. The effects of increase blood pressure or hypertension with more focus on stenosis related to patient specific cases is one of the potential area for numerical investigation. Also, there are very limited studies with clinical relevance which supports that a change of posture will certainly cause symptoms/stroke in patients altered cerebral auto regulation. Due to the risks involved in stroke (plaque rupture) in patients, studies supporting the change of posture in such patients are not possible to investigate clinically. Hence, this kind of observation of minor flow changes in healthy individuals and significant variation in patients with different postures under the influence of altered gravity are demonstrated in this chapter/section using numerical simulation approach. This chapter/section, therefore summarizes the investigation on effects of hypertension in comparison with normal blood pressure on normal and stenosed carotid artery bifurcation. In addition, effects of altered gravity is also discussed during change of posture from sleeping to standing under normal blood pressure condition.

2. Methodology

2.1 FSI theory

The blood flow behavior in both cases (a) and (b) of this study is assumed to be governed by the Navier–Stokes equations of incompressible flows. The fluid domain in FSI simulation is solved using modified momentum equation adopting moving velocity concept along with continuity equation as given in Eq. (1) [2, 11, 12].

$$\frac{\partial}{\partial t}\int_{\Omega}\rho\partial\Omega+\int_{S}\rho(v-v_b)n\partial S=\int_{S}\left(\tau_{ij}i_j-Pi_i\right)n\partial S+\int_{\Omega}b_i\partial\Omega \tag{1}$$

The artery wall is assumed to be elastic, isotropic, incompressible and homogeneous and the transient dynamic structural solution is given by Eq. (2) [4]. The stiffness matrix is updated in each time step and the Newmark method is adopted in updating the displacement terms at each time interval and further the stiffness matrix is solved using direct solver in particular sparse solver for each time step.

$$[M]\{\ddot{U}\}+[C]\{\dot{U}\}+[K]\{U\}=\{F^a\} \tag{2}$$

FSI Algorithm: Based on the Newtonian assumption with incompressible flow for blood and linear elastic property of arterial wall, the two-way transient FSI analysis is performed using system coupling FSI solver in ANSYS-18.0.

This coupling solver solves fluid and solid domain separately using ANSYS CFX and ANSYS STRUCTURAL respectively as shown in the **Figure 1**. The pressure loads obtained from initial ANSYS CFX solution is transferred to the structure through FSI interface and later ANSYS structural domain is solved. Further details of FSI solver are described in [2, 19].

2.2 Modeling

The present study discuss two different patient specific case, (a) healthy and normal carotid bifurcation without any symptoms of stroke and (b) stenosis of 75% at ECA root, while ICA and CCA appears to be normal. The required geometric

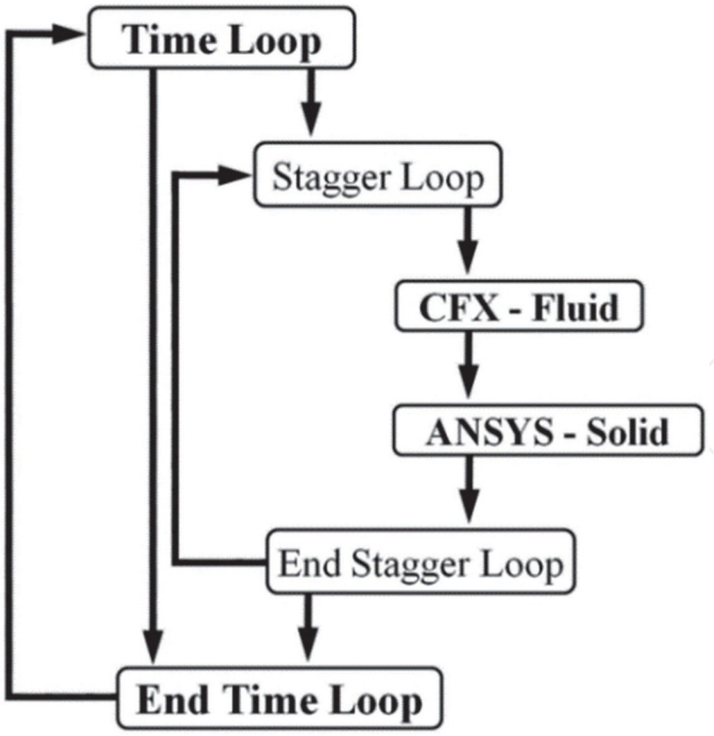

Figure 1.
Fluid structure interaction algorithm in ANSYS.

model is generated based on data obtained from CT angio scan. **Figure 2** shows the different views of CT scan data and the encircled area highlights the location of carotid bifurcation on both left and right side in addition to the 3D geometric model generated in MIMICS. The 3D fluid and solid models of both these cases left and right carotid system are generated using MIMICS-16 based on CT angio data. The solid model is generated using CATIAV5R20.0, versatile geometric modeling software and further transferred to ANSYS 18.0 for the meshing. Case-(a) carotid system consisting of fluid and structural model is meshed with 233,750 and 43,455 hexahedral elements respectively. Similarly, fluid and solid models of case-(b) carotid system is meshed with 254,220 and 41,760 hexahedral elements as shown in the **Figure 3**.

2.3 Analysis

Generally blood is known to be non-Newtonian physiologically, however in the present study, since the focus in on large arteries, Newtonian assumption is acceptable as relatively high shear rate occurs [23]. In medium and smaller arteries, non-Newtonian assumption is valid as shear rate is lower than 100 s^{-1} and shear stresses depend non-linearly on the deformation rate [24]. A time varying velocity pulse is applied at inlet of both the carotid cases based on available literature [8]. A typical inlet velocity profile as shown in the **Figure 4** is applied for both cases (a) and (b) without altered gravity behavior which contributes to sleeping posture. However, under altered gravity condition, such as standing posture, the inlet velocity profile will be as shown in the **Figure 4**. Under the standing posture condition, the inlet velocity will change considering the hydrostatic pressure, which is related to gravity and referred as ρgh, where ρ is fluid density, g is the acceleration due gravity and h is the height of the hydrostatic column [21]. The height of the column of blood is always referred at the level of the heart.

Also, to include the peripheral resistance, a time varying pressure wave form is applied at the outlet as shown in the **Figure 4** [5]. The range of pulse pressure is

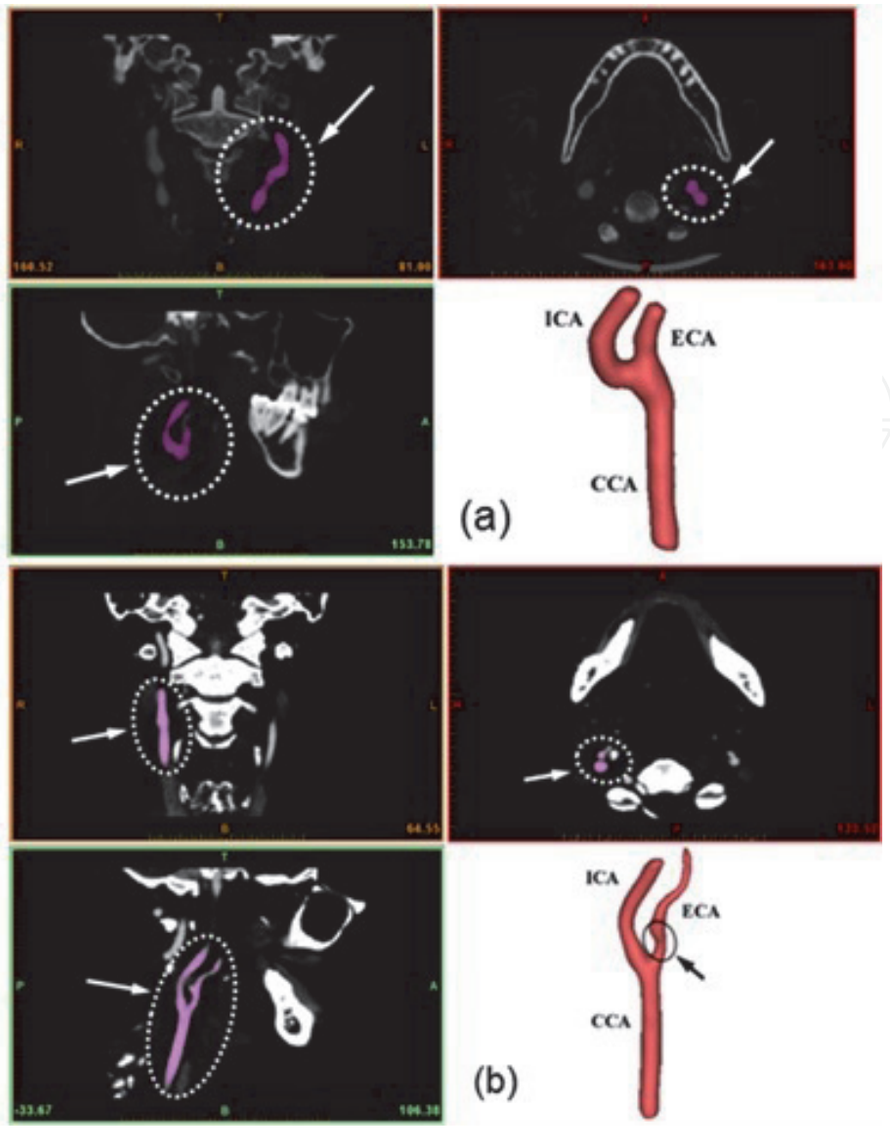

Figure 2.
Different views of CT scan of carotid bifurcation, case-(a) Normal carotid artery model and case-(b) Stenosed carotid artery model.

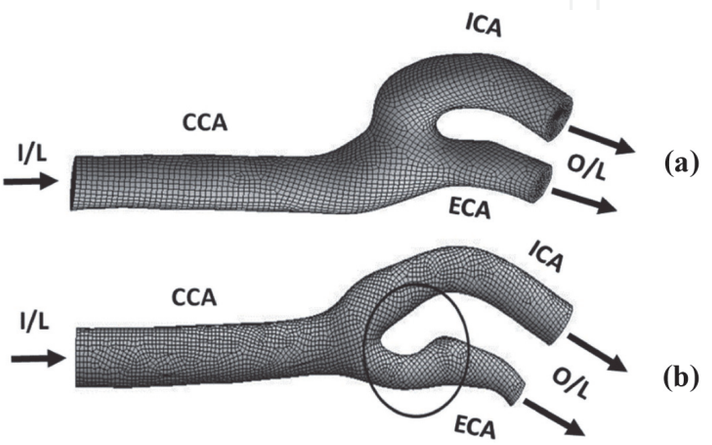

Figure 3.
Meshed model of case (a) Normal carotid bifurcation and (b) Stenosed carotid artery model.

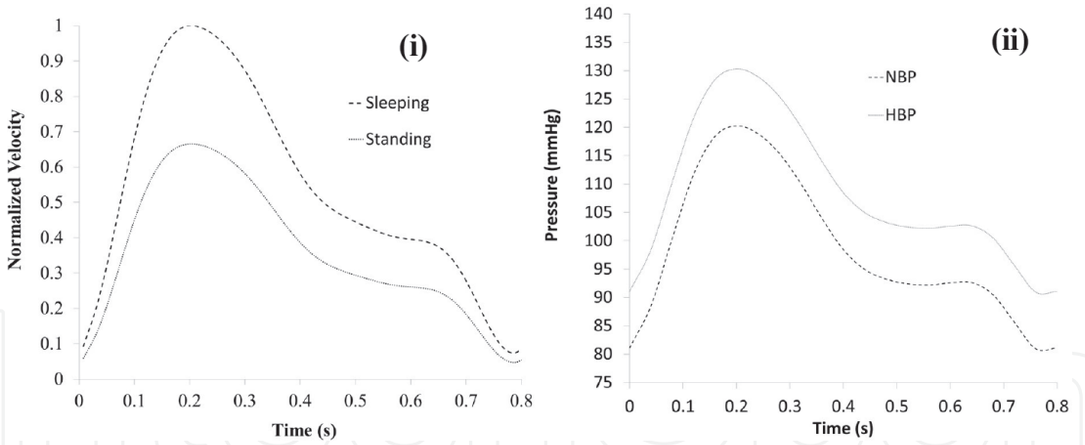

Figure 4.
(i) Normalized inlet velocity waveform and (ii) outlet pressure waveform with NBP and HBP.

different as the simulation is carried out for both NBP and HBP having 80–125 mm Hg and 100–170 mm Hg, respectively. Each pulse cycle for a time period of 0.8 s is discretized into 180 time steps to simulate the flow behavior more accurately. In this study, blood flow properties in form of density and dynamic viscosity are considered to be 1050 kg/m^3 and 0.004 N-sec/m^2 respectively [15]. The arterial wall is assumed to behave linearly-elastic having elastic modulus is 0.9 MPa and Poisson's ratio of 0.40 with density of 1120 kg/m^3 [20, 25]. The convergence criteria of fluid flow and across the fluid-surface interface is set at 10^{-4} and 10^{-3} respectively and low Reynolds k-ω model is used to model the turbulence behavior [22]. In this study, with sleeping position as reference, effects of NBP and HBP on flow behavior are investigated and further altered gravity evaluation is performed for change of posture from sleeping to standing under NBP condition. These simulation results provide useful data in quantifying the hemodynamic changes during different blood pressures (NBP and HBP) and also during change of posture from sleeping to standing.

3. Results and discussion

Numerical simulation in this study of both the cases (a) and (b) is carried out for 3 pulse cycle and results obtained in the last cycle is considered for the investigation. The hemodynamic parameters like velocity, WSS and arterial wall deformation are studied at specific instants of pulse cycle like peak systole (i), early systole (ii) and late diastole (iii). Inlet velocity is considered with reference to sleeping position and effects of variation in pressure parameter is investigated under NBP and HBP conditions. Under altered gravity assumption, inlet velocity is considered for change of position from sleeping to standing under NBP condition only. Flow behavior will be less intense during standing posture in contrast to sleeping condition. WSS is considered to be the most crucial and interesting hemodynamic parameters related to the atherosclerotic progression. It varies with time due to the pulsatility of the flow waveform and the maximum value generally occurs at the peak systole when the inflow is maximum.

Velocity: The velocity streamlines of the case (a) normal carotid bifurcation subjected to NBP & HBP is shown in **Figure 5**. In this case, higher velocity magnitude is observed at peak systole for all the blood pressure models. Flow recirculation region is almost similar at peak systole and early diastole, however, in late diastole, it is more chaotic at the carotid bulb.

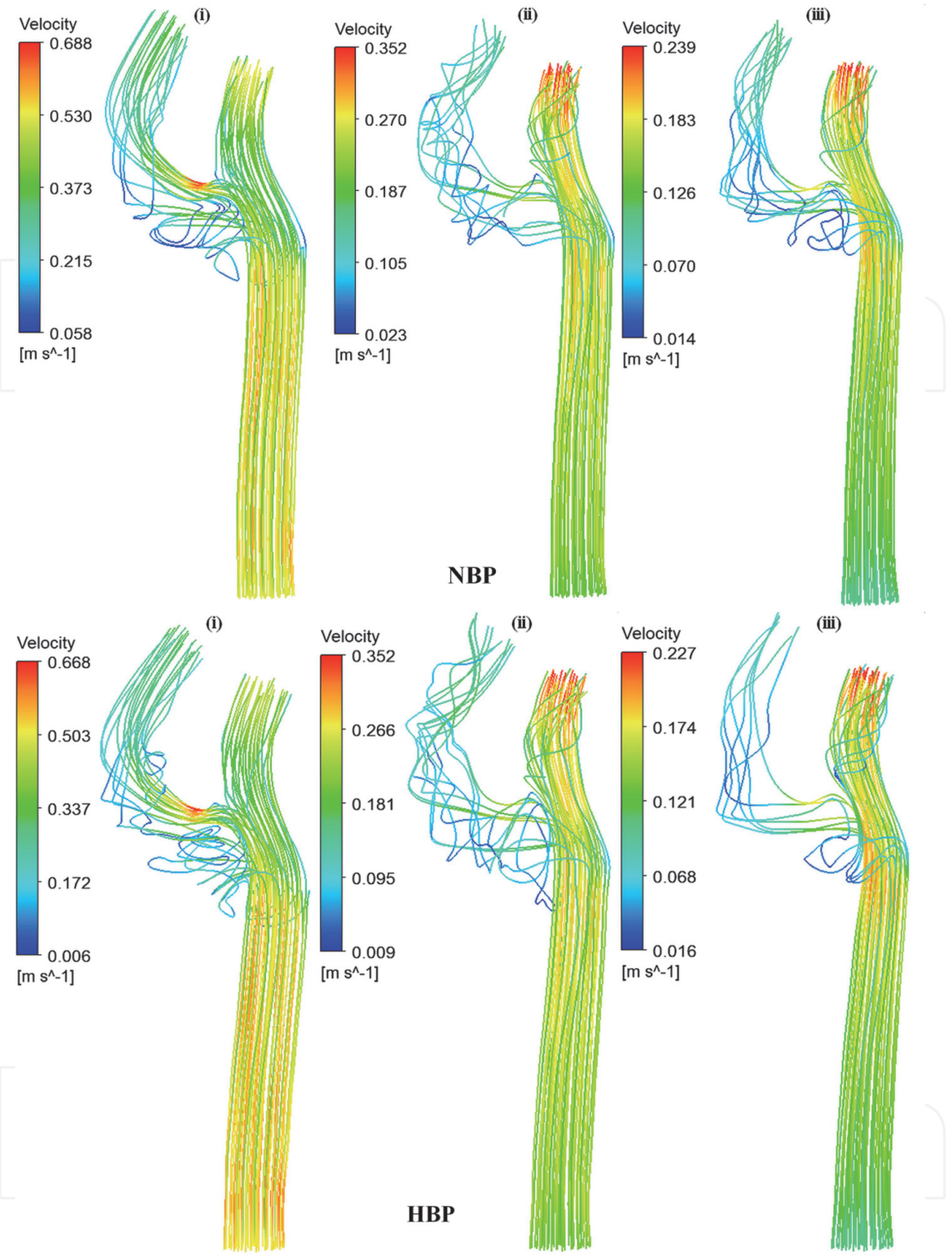

Figure 5.
Velocity streamline plot for case (a): Normal carotid artery model under NBP & HBP during (i) peak systole, (ii) early systole (iii) late diastole.

High-velocity gradients is seen at the bifurcation and flow reversals along the outer wall of the ICA due to bifurcation of the arterial geometry and carotid bulb is located at the outer wall region of the ICA leading to flow reversals. Similar behavior is observed with higher blood pressure. As compared to NBP, streamlines tends to be more laminar at higher blood pressure. The flow separation was observed to be leading to vortices and the vortex shedding was observed at elevated flow rates due to the increased momentum of flow. At peak systole, higher velocity was observed, and flow separation was occurring at the upper portion of the CCA due to

bifurcation and due to sudden increase in diameter at carotid sinus. The velocity magnitude was inversely proportional to the variation in blood pressure. This was due to higher peripheral resistance due to blood pressure, which also leads to an increase in arterial deformation. The velocity is higher in the ECA as compared to the ICA due to the geometry, where the centerline of is almost in line with the CCA. In case (b) of stenosed carotid artery model, the flow is almost similar at peak systole, except minor flow recirculation areas at the carotid sinus and post stenotic region in in ECA which gets magnified with the increase in the blood pressure as shown in the **Figure 6**. However, at early diastole and late diastole, the flow turns chaotic post stenosis and at the carotid sinus. The stenosis further induces abrupt flow disturbance creating complex vortex formation in the downstream of the narrowed ECA.

The vortex induced in the downstream is highly complex and extends till the distal end of the ECA and more prominent in the later part of the cardiac cycle. The magnitude of the velocity is reduced with an increase in blood pressure at peak systole and it tends to increase at late diastole at ICA. The flow recirculation region

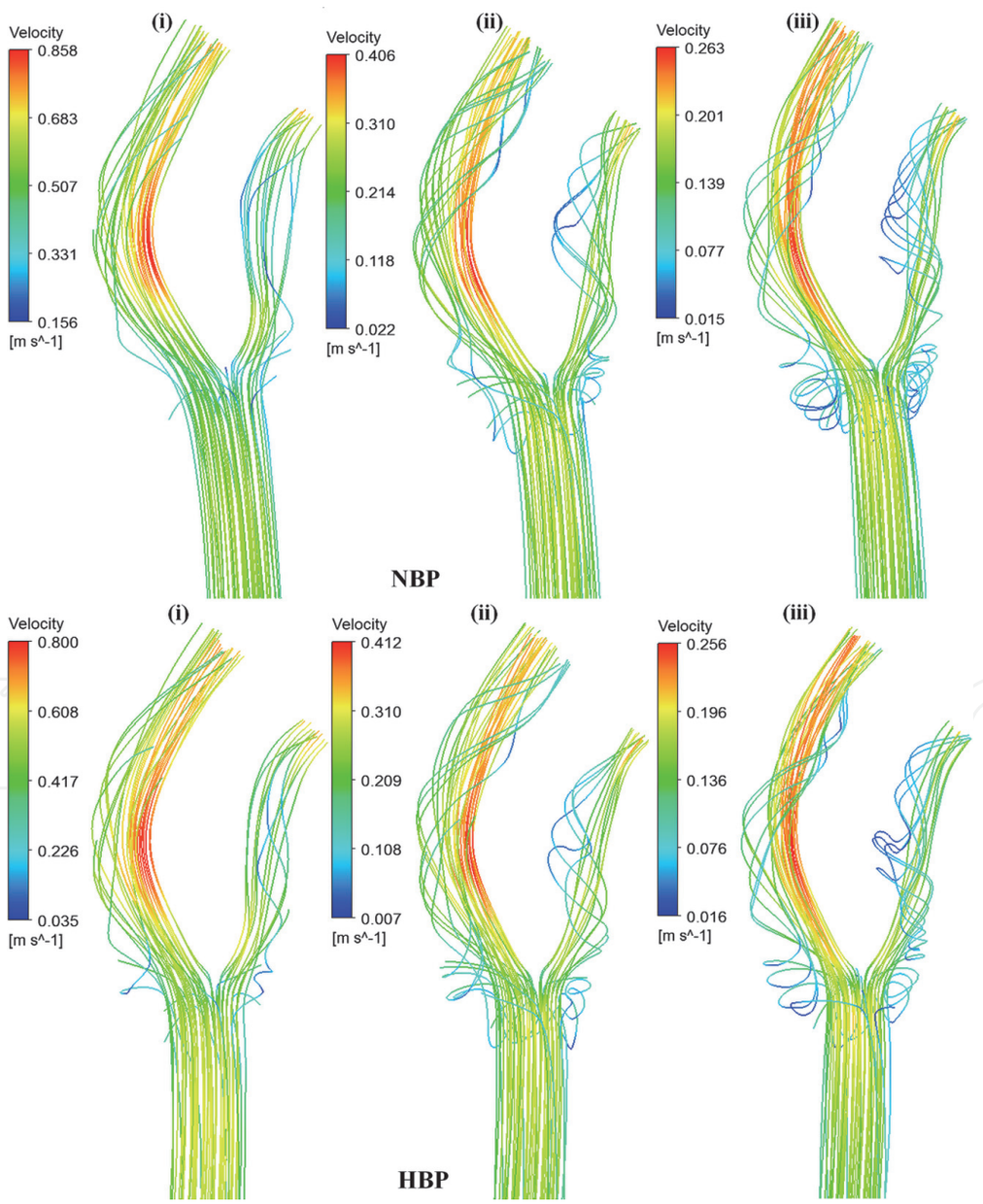

Figure 6.
Velocity streamline plot for case (b): Stenosed carotid artery model under NBP & HBP during (i) peak systole, (ii) early systole (iii) late diastole.

is increased with higher blood pressure at late diastole. Under the altered gravity, the hemodynamic characteristics in both cases (a) and (b) will be similar to that as observed during sleeping posture. However, the flow will be less intense during standing posture in contrast to sleeping condition. The flow changes observed during sleeping and standing in case-(a) and (b) is plotted in the **Figure 7**. With the change of posture from sleeping to standing, the velocity changes abruptly in both these cases as shown in the **Figure 7** with similar pattern. In case (a), the velocity in standing position decreases 25 to 30% with mild variation in flow separation. However, in case (b), the variation in magnitude of flow velocity shows the elevated velocities as compared to case (a). The percentage variation of flow velocity during the change of posture from sleeping to standing indicates a drop in 30–35%, as observed in the **Figure 7**.

Wall Shear Stress: Wall shear stress is a significant parameter as it is related to degeneration of the arterial wall. **Figure 8** shows the WSS contours at peak systole, early and late diastole phase of the cardiac cycle in case (a) normal carotid artery. Maximum WSS is observed at NBP and varies inversely with blood pressure and the lowest WSS magnitude is observed at HBP. In both NBP and HBP cases, the WSS is concentrated at the bifurcation point towards the inner wall at the stagnation point due to high velocity gradient. The low WSS at the outer wall of the ICA at the bifurcation decreases with the increase in blood pressure. At peak systole the flow separation occurs at the base of the bifurcation near the carotid sinus leading to lower WSS and leading along the outer wall of the ICA at late diastole.

Significantly lower WSS is observed at late diastole where the flow recirculation is maximum. The decrease in WSS is due to reduced flow velocity and enlargement of the arterial wall due to increased blood pressure. **Figure 8** shows the WSS contours for NBP and HBP at different phases of the cardiac cycle in case (b) of stenosed carotid artery model. Maximum WSS magnitude at peak systole for NBP, HBP are 10.147 Pa, 10.176 Pa respectively. The WSS tends to concentrate mainly near the stenosis region at the bifurcation and at the inner wall of the ICA.

At peak systole, the WSS is concentrated mainly at the inner wall of the ICA at the curved region, whereas the low WSS region is predominant immediately after the stenosis for both BP cases. The intensity of low shear region increases at early diastole and it spreads all over the inner wall of ECA at late diastole. The inner wall of the ECA at the bifurcation zone have traces of low WSS (>2 Pa) which have slightly reduced influence of progression of atherosclerosis [19]. In addition, at this instant WSS increases pre stenosis at the neck of the stenosis. Low WSS is also observed at the carotid sinus and post stenosis regions in the ECA due to flow recirculation caused by sudden increase in diameter. This low WSS (>0.4 Pa)

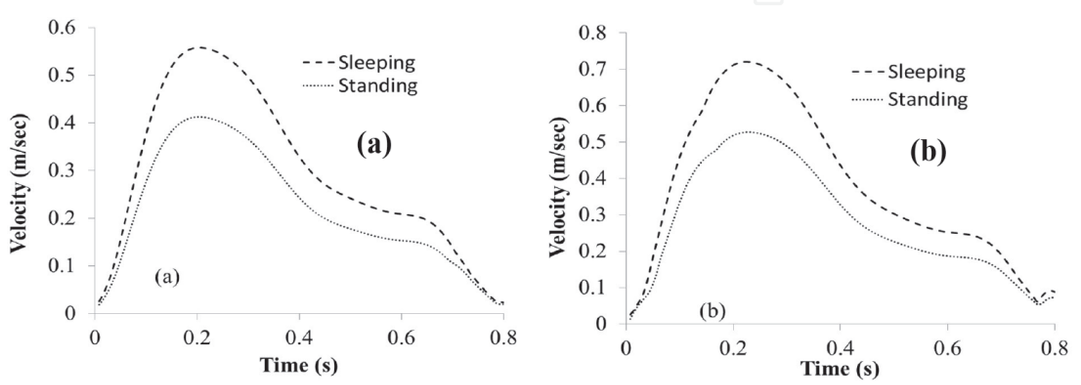

Figure 7.
Comparison of velocity during of change of posture from sleeping to standing in case (a) and case (b) in NBP condition.

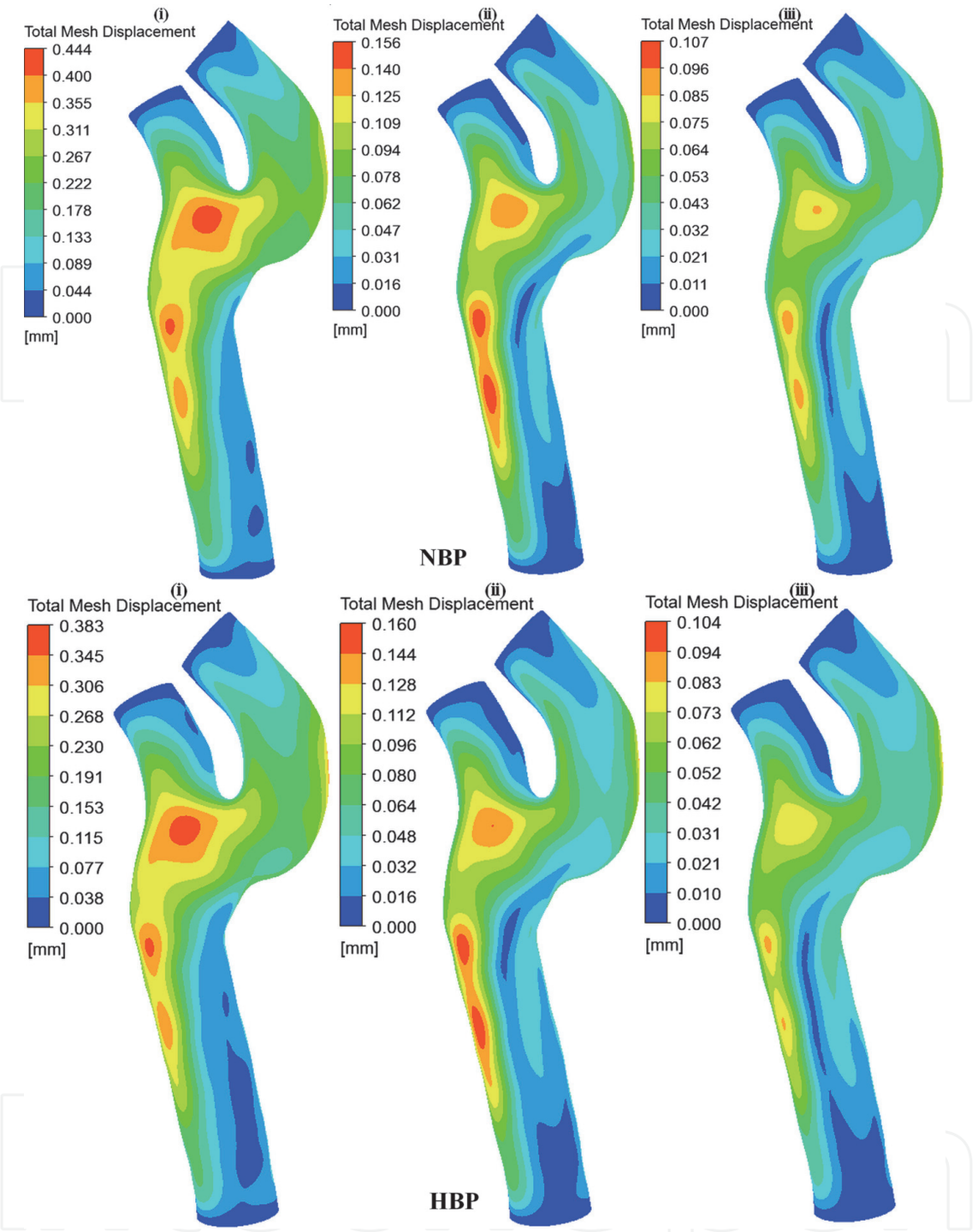

Figure 8.
WSS contour plot for case (a): Normal carotid artery model under NBP & HBP during (i) peak systole, (ii) early systole (iii) late diastole.

encourage the progression of atherosclerosis. The low WSS region is at the neck of the bifurcation below the carotid sinus where there is maximum flow recirculation. The low WSS at higher BP will certainly trigger atherosclerosis progression and endothelial cell disorientation [22] (**Figure 9**).

Even though the WSS pattern across the carotid models in both cases (a) and (b) will be similar to that of sleeping condition, however, during the change of posture from sleeping to standing, due to less flow, the maximum variation in WSS is observed during peak systole as compared to rest of the pulse cycle. WSS changes observed in both these cases (a) and (b) are compared in the **Figure 10** through the entire pulse cycle. The change of posture from sleeping to standing drops the WSS

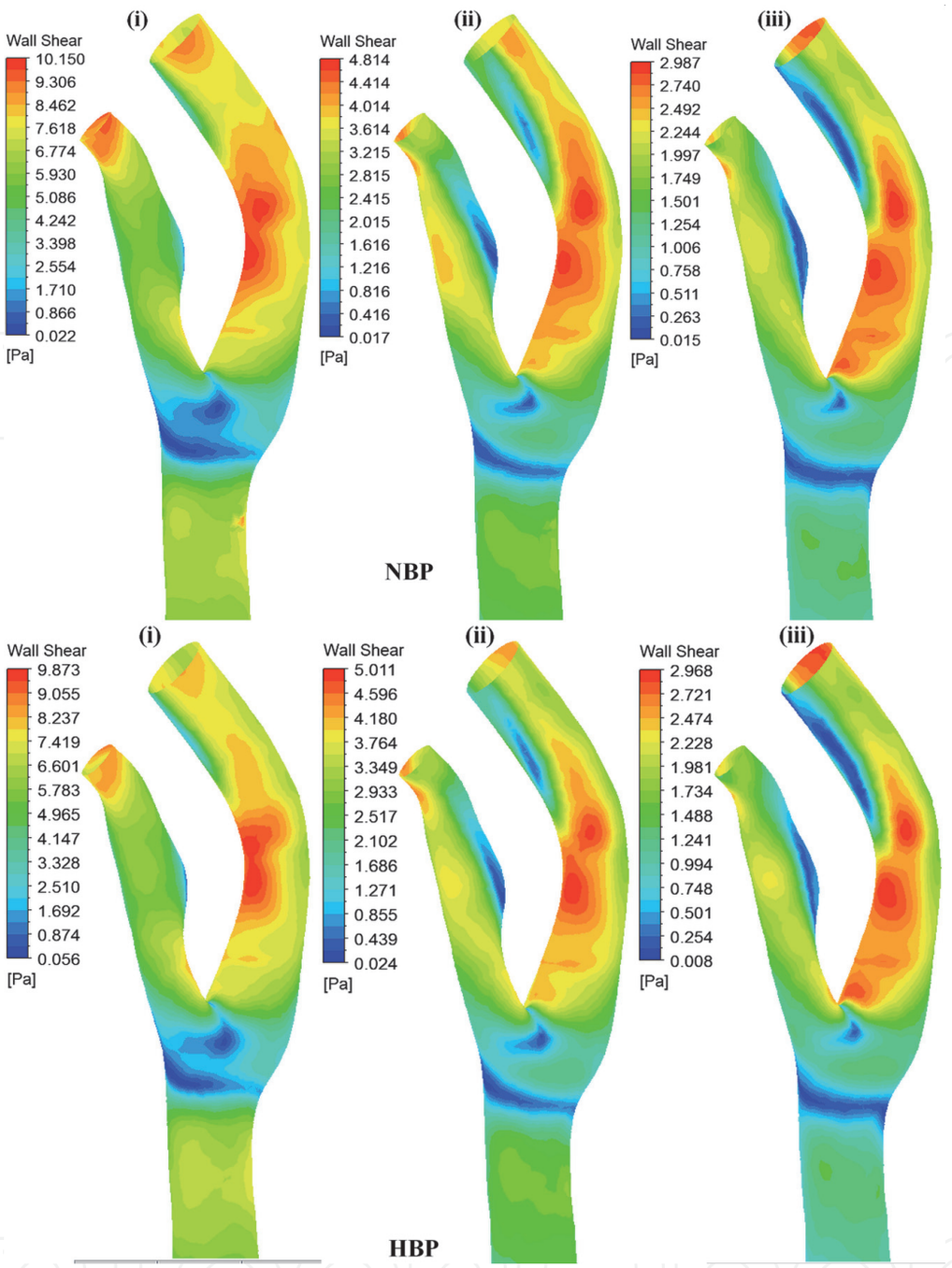

Figure 9.
WSS contour plot for case (b): Stenosed carotid artery model under NBP & HBP during (i) peak systole, (ii) early systole (iii) late diastole.

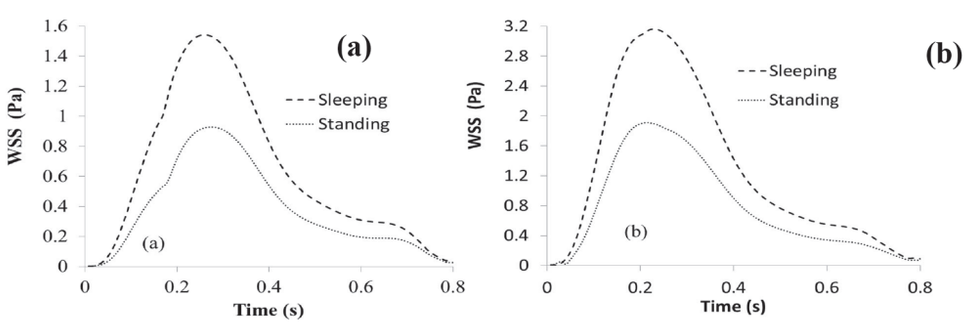

Figure 10.
Comparison of WSS during of change of posture from sleeping to standing in case (a) and case (b) in NBP condition.

by 40–45%, as observed in case (a). The WSS is found to be less disturbed without any major complexity due to normal flow behavior. In case (b), the WSS variation as compared for case (a) substantially drop by 50% during the change of posture from sleeping to standing. Significant WSS variation during the change of postures will certainly trigger the damage to arterial wall and induce the plaque rupture [26].

Wall Deformation: Figure 11 shows the arterial wall deformation contours at normal carotid artery of case (a) at different phases of the cardiac cycles. The maximum deformation is at the bifurcation region, mainly at the base of the branching of ICA and ECA due to reduced arterial stiffness because of the curvature. Generally, maximum deformation is at the location where the pressure is maximum, especially at the apex of the bifurcation. The curvature of the

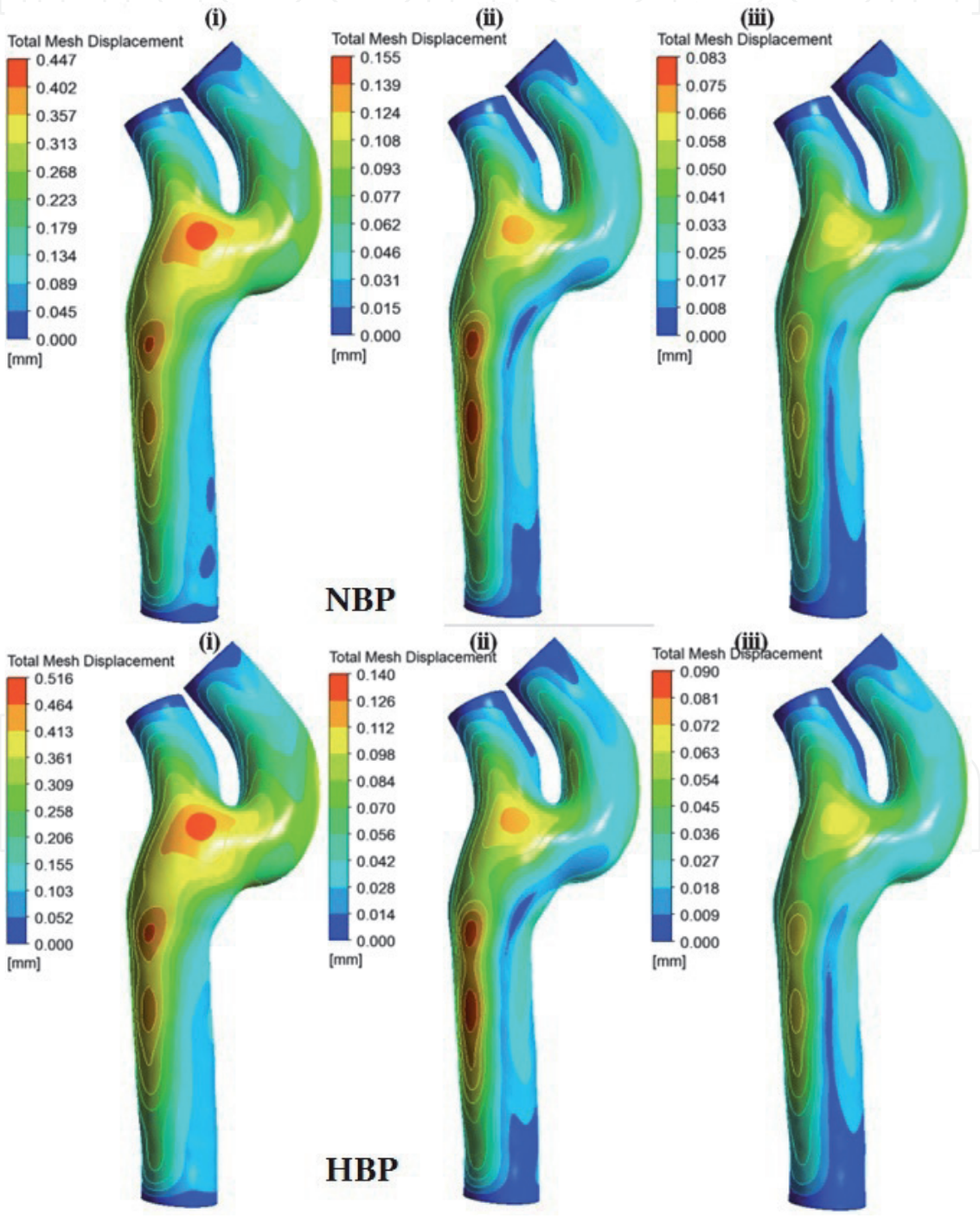

Figure 11.
WSS contour plot for case (a): Normal carotid artery model under NBP & HBP during (i) peak systole, (ii) early systole (iii) late diastole.

bifurcation reduces the stiffness of the wall, and therefore have high wall deformation [27]. The outer wall of the ICA is also subjected to moderate deformations along with the bifurcation region. Low WSS along with higher wall deformation is one of the possible causes of atherosclerosis development. Maximum deformation of 0.447 mm, 0.516 mm, is observed at peak systole for NBP, and HBP conditions respectively.

The maximum arterial deformation occurs at peak systole as observed in the stenosed carotid bifurcation of case (b) as shown in **Figure 10** for both the NBP and HBP conditions. The location of the maximum deformation is observed to be in the bifurcation region. The plaque at the root of the ECA has higher stiffness resulting in reduced elastic deformation. The reduced wall stiffness is localized around the ECA resulted in reduced wall deformation across the stenosed location. Another observation is post stenotic deformation in distal side of the ECA because of eccentric stenosis with a lower profile due to increased stiffness of the plaque. The partial restriction offered for the flow in the ECA diverts the flow through the ICA. However, the increased pressure in the upstream of the narrowed region to compensate the flow has increased the deformation distribution. Therefore, the

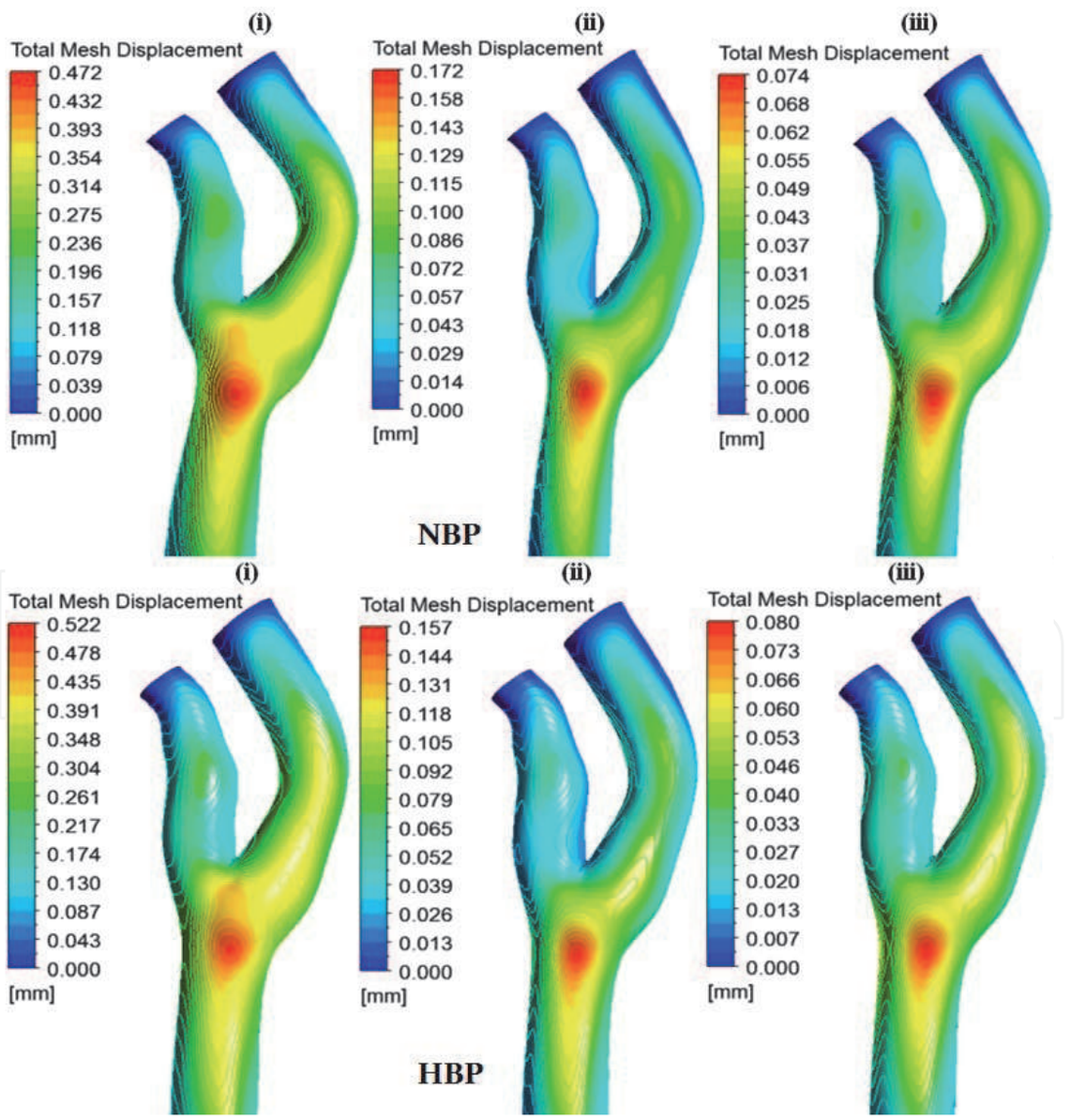

Figure 12.
WSS contour plot for case (b): Stenosed carotid artery model under NBP & HBP during (i) peak systole, (ii) early systole (iii) late diastole.

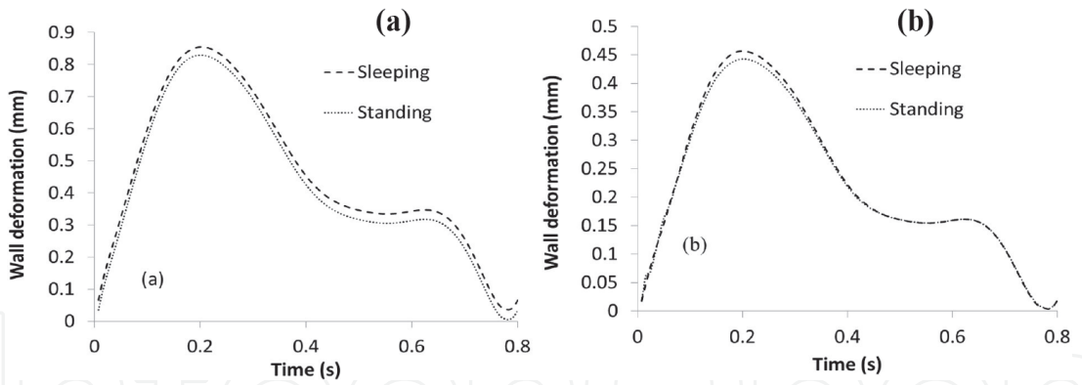

Figure 13.
Comparison of WSS during of change of posture from sleeping to standing in case (a) and case (b) in NBP condition.

maximum deformation is during the peak systole at the entrance of the ICA in the bifurcation region. The deformation profile is typical of normal carotid bifurcation as observed in published literature [28]. There is no significant difference in arterial deformation between the rheological models considered in the study (**Figure 12**).

The variation in wall deformation behavior throughout the pulse cycle during change of postures from sleeping to standing in both the case-(a) and (b) is shown in the **Figure 13**. There is no remarkable difference among sleeping and standing postures in both these cases [29]. The change of position from sleeping to standing notices a drop of less than 5% and 8% as observed for both case (a) and (b) [13, 30]. The obtained deformation pattern shows considerable change during different postures and agrees well with the clinical observation [31]. The high pressure in upstream of stenosis causes the maximum wall deformation and the intense pressure drop at the throat region will result in wall collapse.

4. Conclusion

In this study, the pulsatile flow of blood with different physiological pressure conditions and altered gravity was studied. In normal carotid bifurcation case (a) during both NBP and HBP cases, the curvature of the bifurcation has influenced in reducing the stiffness of the wall resulting in higher wall deformation. The outer wall of the ICA is also subjected to moderate deformations along with the bifurcation region. The WSS is found to be concentrated at the bifurcation and intense flow separation at this zone resulting in lower WSS. However, in case (b), stenosis at the root of the ECA has higher stiffness resulting in reduced elastic deformation. The reduced wall stiffness is localized around the ECA resulted in reduced wall deformation across the stenosed location. Another observation is post stenotic deformation in distal side of the ECA because of eccentric stenosis with a lower profile due to increased stiffness of the plaque. The WSS tends to concentrate mainly near the stenosis region at the bifurcation and at the inner wall of the ICA. The low WSS region is predominant in post stenotic region for both NBP and HBP cases. In both the cases (a) and (b), low WSS at different regions of carotid bifurcation shall significantly influences the progression of atherosclerosis. Under the altered gravity, case-1, demonstrated typical flow behavior as that of normal carotid bifurcation, but minor variations are present due to tortuous bifurcation. It is clear from the results that the wall deformation has dropped by less than 5% during standing posture. However, velocity and WSS show a considerable drop of 25% and 45%

respectively during standing. In case (b), the velocity and WSS drops by 30–35% and 50% while the arterial wall deformation reduces by 8% in standing posture. The moderately higher WSS at the level of maximum stenosis has slightly reduced the arterial wall stiffness resulting in low risk factor of disease progression during standing posture. It can be concluded that risk factors are quite low and the flow behavior is also within the physiological limits, during the change of postures from sleeping to standing. Further, the results of this study demonstrate the potential of numerical simulation in understanding of the causes of atherosclerosis and pave the way in developing innovative computational solutions to aid the early diagnosis of atherosclerosis.

Acknowledgements

Authors thanks Department of Radio-Diagnosis and Imaging, Kasturba Hospital, Manipal for providing the patient specific data to carry out the numerical simulation.

Conflict of interest

The authors declare no conflict of interest.

Abbreviations and nomenclature

CCA	Common Carotid Artery
ICA	Internal Carotid Artery
ECA	External Carotid Artery
NBP	Normal Blood Pressure
HBP	High Blood Pressure
WSS	Wall Shear Stress
FSI	Fluid Structure Interaction
ρ	Density
τ	Stress tensor
v	Velocity vector
v_b	Grid velocity
P	Pressure
b_i	Body force at time t
M	Structural mass matrix
C	Structural damping matrix
K	Structural stiffness matrix
F^a	Applied load vector
$\ddot{U}$	Acceleration component
$\dot{U}$	Velocity
U	Displacement vector

Author details

S.M. Abdul Khader, Nitesh Kumar and Raghuvir Pai*
Department of Mechanical and Manufacturing Engineering, Manipal Institute of Technology, Manipal Academy of Higher Education, Manipal, India

*Address all correspondence to: raghuvir.pai@manipal.edu

References

[1] Hosseini V, Mallone A, Mirkhani N, Noir J, Salek M, Pasqualini FS, et al. A Pulsatile Flow System to Engineer Aneurysm and Atherosclerosis Mimetic Extracellular Matrix. Adv Sci. 2020; 2000173.

[2] Jiang F, Zhu Y, Gong C, Wei X. Atherosclerosis and Nanomedicine Potential: Current Advance and Future Opportunities. Curr Med Chem. 2020;

[3] Michail M, Davies JE, Cameron JD, Parker KH, Brown AJ. Pathophysiological coronary and microcirculatory flow alterations in aortic stenosis. Nat Rev Cardiol. 2018;15 (7):420–31.

[4] Yang H, Yu PK, Cringle SJ, Sun X, Yu D-Y. Microvascular network and its endothelial cells in the human iris. Curr Eye Res. 2018;43(1):67–76.

[5] Wang R, Yu X, Zhang Y. Mechanical and structural contributions of elastin and collagen fibers to interlamellar bonding in the arterial wall. Biomech Model Mechanobiol. 2020;1–14.

[6] Pai R, Khader SM, Ayachit A, Ahmad KA, Zubair M, Rao VRK, et al. Fluid-Structure Interaction Study of Stenotic Flow in Subject Specific Carotid Bifurcation—A Case Study. J Med Imaging Heal Informatics. 2016;6(6):1494–9.

[7] Rayz VL, Cohen-Gadol AA. Hemodynamics of Cerebral Aneurysms: Connecting Medical Imaging and Biomechanical Analysis. Annu Rev Biomed Eng. 2020;22.

[8] Kumar N, Khader SMA, Pai R, Khan SH, Kyriacou PA. Fluid structure interaction study of stenosed carotid artery considering the effects of blood pressure. Int J Eng Sci [Internet]. 2020; 154:103341. Available from: http://www.sciencedirect.com/science/article/pii/S0020722520301294

[9] Yang JW, Im Cho K, Kim JH, Kim SY, Kim CS, You GI, et al. Wall shear stress in hypertensive patients is associated with carotid vascular deformation assessed by speckle tracking strain imaging. Clin Hypertens. 2014;20(1):10.

[10] Samaee M, Tafazzoli-Shadpour M, Alavi H. Coupling of shear–circumferential stress pulses investigation through stress phase angle in FSI models of stenotic artery using experimental data. Med Biol Eng Comput. 2017;55(8):1147–62.

[11] Rabby MG, Razzak A, Molla MM. Pulsatile non-Newtonian blood flow through a model of arterial stenosis. Procedia Eng [Internet]. 2013;56:225–31. Available from: http://dx.doi.org/10.1016/j.proeng.2013.03.111

[12] Abdul Khader SM, Ayachit A, Pai R, Zubair M, Ahmed KA, Rao VR. Study of the influence of Normal and High Blood pressure on normal and stenosed Carotid Bifurcation using Fluid-Structure Interaction. In: Applied Mechanics and Materials. 2013. p. 982–6.

[13] Azran A, Hirao Y, Kinouchi Y, Yamaguchi H, Yoshizaki K. Variations of the maximum blood flow velocity in the carotid, brachial and femoral arteries in a passive postural changes by a Doppler ultrasound method. In: The 26th Annual International Conference of the IEEE Engineering in Medicine and Biology Society. 2004. p. 3708–11.

[14] Alirezaye-Davatgar MT. Numerical simulation of blood flow in the systemic vasculature incorporating gravitational force with application to the cerebral circulation. University of New South Wales; 2006.

[15] Gisolf J, others. Postural changes in humans: effects of gravity on the circulation. 2005.

[16] Kim CS, Kiris C, Kwak D, David T. Numerical simulation of local blood flow in the carotid and cerebral arteries under altered gravity. 2006;

[17] Mittal R, Seo JH, Vedula V, Choi YJ, Liu H, Huang HH, et al. Computational modeling of cardiac hemodynamics: current status and future outlook. J Comput Phys. 2016;305:1065–82.

[18] Carpenter HJ, Gholipour A, Ghayesh MH, Zander AC, Psaltis PJ. A review on the biomechanics of coronary arteries. Int J Eng Sci. 2020;147:103201.

[19] Wong KKL, Wang D, Ko JKL, Mazumdar J, Le T-T, Ghista D. Computational medical imaging and hemodynamics framework for functional analysis and assessment of cardiovascular structures. Biomed Eng Online. 2017;16(1):35.

[20] Hirschhorn M, Tchantchaleishvili V, Stevens R, Rossano J, Throckmorton A. Fluid–structure interaction modeling in cardiovascular medicine–A systematic review 2017–2019. Med Eng Phys. 2020;

[21] Al-Sharea A, Lee MKS, Whillas A, Michell DL, Shihata WA, Nicholls AJ, et al. Chronic sympathetic driven hypertension promotes atherosclerosis by enhancing hematopoiesis. Haematologica. 2019;104(3):456–67.

[22] Sun HT, Sze KY, Tang AYS, Tsang ACO, Yu ACH, Chow KW. Effects of aspect ratio, wall thickness and hypertension in the patient-specific computational modeling of cerebral aneurysms using fluid-structure interaction analysis. Eng Appl Comput Fluid Mech. 2019;13(1): 229–44.

[23] Perktold K, Peter R, Resch M. Pulsatile non-Newtonian blood flow simulation through a bifurcation with an aneurysm. Biorheology. 1989;26(6): 1011–30.

[24] Khader SMA, Azriff A, Johny C, Pai R, Zuber M, Ahmad KA, et al. Haemodynamics Behaviour in Normal and Stenosed Renal Artery using Computational Fluid Dynamics. J Adv Res Fluid Mech Therm Sci. 2018;51(1): 80–90.

[25] Dhawan SS, Nanjundappa RPA, Branch JR, Taylor WR, Quyyumi AA, Jo H, et al. Shear stress and plaque development. Expert Rev Cardiovasc Ther [Internet]. 2010;8(4):545–56. Available from: https://www.ncbi.nlm.nih.gov/pmc/articles/PMC5467309/pdf/nihms213759.pdf

[26] Ku DN. Blood flow in arteries. Annu Rev Fluid Mech. 1997;29(1): 399–434.

[27] Zhao SZ, Xu XY, Hughes AD, Thom SA, Stanton A V, Ariff B, et al. Blood flow and vessel mechanics in a physiologically realistic model of a human carotid arterial bifurcation. J Biomech. 2000;33(8):975–84.

[28] Toloui M, Firoozabadi B, Saidi MS. A numerical study of the effects of blood rheology and vessel deformability on the hemodynamics of carotid bifurcation. Sci Iran [Internet]. 2011; 19(1):119–25. Available from: http://dx.doi.org/10.1016/j.scient.2011.12.008

[29] Toloui M, Firoozabadi B, Saidi MS. A numerical study of the effects of blood rheology and vessel deformability on the hemodynamics of carotid bifurcation. Sci Iran [Internet]. 2012;19(1):119–26. Available from: http://dx.doi.org/10.1016/j.scient.2011.12.008

[30] Kim CS, Kiris C, Kwak D, David T. Numerical Simulation of Local Blood Flow in the Carotid and Cerebral Arteries Under Altered Gravity. J Biomech Eng [Internet]. 2006;128(2): 194. Available from: http://biomechanical.asmedigitalcollection.asme.org/article.aspx?articleid=1415462

[31] Savin E, Bailliart O, Checoury A, Bonnin P, Grossin C, Martineaud J-P. Influence of posture on middle cerebral artery mean flow velocity in humans. Eur J Appl Physiol Occup Physiol. 1995; 71(2–3):161–5.